coatings

MDPI

Article

Calculation of Stress Intensity Factor for Annular Double Cracks on Inner Surface of Pipeline

Jintai Cui, Huifang Li *, Zhiwei Wu and Caifu Qian

College of Mechanical and Electrical Engineering, Beijing University of Chemical Technology, Beijing 100029, China; jerrycui2022@163.com (J.C.); zwzhiweiwu@163.com (Z.W.); qiancf@mail.buct.edu.cn (C.Q.)
* Correspondence: lihf@mail.buct.edu.cn

Abstract: Cracks in engineered pipelines often appear in the form of multiple cracks or crack clusters with interactions between them. It is important to study the interaction between cracks if the pipeline crack cluster is to be evaluated in terms of equivalence and safety assessment. In this paper, based on FRANC3D crack analysis software, the interaction between circumferential parallel double cracks on the inner surface of pipelines was investigated, the factors affecting the interaction were examined, and the empirical equations for calculating the stress intensity factor (SIF) of double cracks was proposed. The results show that if there is no bias between the double cracks, the crack leading edge is shielded, but if there is offset between the double cracks, the crack leading edge is subjected to different interactions at different locations. The distal end of the cracks is generally strengthened, while the proximal end of the cracks is probably more shielded. The interaction effects between cracks are dependent on their relative positions rather than the pipe size or concerned crack size. According to the numerical simulation, boundaries for shielding or enhancing interactions were obtained, and the stress intensity factor calculation equations were fitted.

Keywords: double crack in pipelines; stress intensity factor; interaction between cracks

Citation: Cui, J.; Li, H.; Wu, Z.; Qian, C. Calculation of Stress Intensity Factor for Annular Double Cracks on Inner Surface of Pipeline. *Coatings* **2024**, *14*, 744. https://doi.org/10.3390/coatings14060744

Academic Editor: Alexander Tolstoguzov

Received: 28 April 2024
Revised: 6 June 2024
Accepted: 7 June 2024
Published: 12 June 2024

1. Introduction

In petrochemical, aerospace, and other industries, the application of pressure piping is very extensive, and the safe operation of piping is one of the key factors affecting the normal operation of equipment. In reality, cracks may exist on the pipeline and may even be in the form of multi-cracks or crack groups due to processing, welding, corrosion, etc. [1]. As the direct abandonment of the pipeline containing cracks is unscientific and uneconomical, it is necessary to analyze the impact of cracks on pipeline safety. Irwin [2] in 1957 proposed the stress intensity factor theory, which lays the foundation for crack research.

At present, there are a lot of studies on single cracks in pipelines [3–15], but pipeline cracks often appear in the form of multiple cracks or crack groups. For multiple cracks, the study of crack interactions is of great significance. Many scholars have conducted more mature studies on double cracks on flat plates or other structures. Tanwar et al. [16] investigated the problem of antiplane stress at the interface of a composite material and obtained the variation in the stress intensity factor at the crack tip for three cracks with different crack lengths and different material combinations. Anis et al. [17] studied the problem of double cracking in flat plates, examined the factors affecting the interaction between double cracks, and gave a formula for calculating the double crack stress intensity factor. Shen et al. [18] used the complex function method and the integral method to calculate the stress intensity factor of parallel multi-cracks, analyzed the interaction mechanism between multi-cracks, and obtained the relative positions of cracks subject to enhancement or shielding. Wang et al. [19] proposed a new method to study multi-crack interactions based on the extended finite element method for calculating multi-crack stress intensity factors and predicting the direction of crack extension. Hoang et al. [20] examined the effect of crack interactions on

SIFs based on experimental observations and finite element analysis and gave a formula for calculating the multi-crack stress intensity factor. Parsania et al. [21] utilized ABAQUS finite element analysis software for double cracks in infinitely large flat plates to investigate the effect of the location of the auxiliary cracks on inter-crack interactions. Han [22] studied the interactions between flat plate cracks, obtained the relative position distribution of parallel biased double cracks subjected to shielding action or enhancement, and defined and fitted the stress intensity factor correction coefficients. Zhang et al. [23] studied the interaction between non-parallel double cracks and obtained the change rule of the stress intensity factor with an inclination angle. Using the boundary element method, for the flat plate containing multi-cracks under tensile load, Huang et al. [24] investigated the boundary element method, for the flat plate containing multi-cracks under tensile load, to study the influence of multi-crack angle, length, distribution location, and spacing on the inhibition and enhancement effect. Based on the numerical simulation method of the virtual crack closure technique (VCCT), Cui et al. [25] investigated the effect of inter-crack spacing and size on the inter-crack interactions for double crack interactions in pipeline welds. Based on the 3D virtual crack closure technology (3D-VCCT), Yao et al. [26] studied the effect of auxiliary crack location and size on the stress intensity factor of the leading edge of the main crack. Hamzah et al. [27] investigated the multi-crack interactions in bonded dissimilar materials, and the results showed that the crack stress intensity factor depends largely on the elastic constants ratio, crack size, crack spacing and size, and the crack stress intensity factor, crack geometry, the distance between each crack, and the distance between the crack and the boundary. It is found from the above review that there are extensive examinations on the factors affecting the interactions between flat plate cracks, and as a result, formulas or models are proposed to quantitatively characterize the interactions between flat plate cracks.

Considering structure and application conditions, there are big differences between pipes and flat plates, so scholars also carried out studies on pipeline cracking problems. Xie et al. [28] proposed a fatigue crack extension method for pipelines with corrosion defect interactions and analyzed the interaction mechanism between cracks and corrosion defects. Sahnoun et al. [29] examined the effect of spacing on inter-crack interactions and showed that inter-crack interactions are very significant when the relative distance is less than 0.3, and vice versa, the interactions can be neglected. Chong et al. [30] investigated the effects of double crack spacing and relative size between cracks on the stress intensity factor of annular double cracks in pipelines through finite element analysis software for the interaction between multiple cracks in submarine pipelines. He et al. [31] studied the effect of the axial double crack angle on the stress intensity factor of pipelines, and the results showed that the increase in the angle between double cracks would make the stress intensity factor increase and the expansion rate increase. Yu et al. [32] studied the influence of the angle and distance between double cracks and the angle between cracks and the pipe axis on the fatigue life of submarine pipelines, and the results showed that the fatigue life of pipelines and cracks are negatively correlated with the angle of the pipe axis. Li et al. [33] and Wei et al. [34] investigated the effect of axial multi-cracks on the strength of pipelines, and the results showed that for pipelines containing double axial cracks, the stress superposition effect between cracks is gradually weakened with the increase in the spacing between double cracks, and the interaction between the cracks can be ignored when the spacing is greater than a certain value. Qin et al. [35] studied the influence law between two axial cracks in thick-walled cylinders and proved that there is a critical value for the interaction between cracks. Zhang et al. [36] investigated the effects of crack geometry, relative position, and internal pressure on the cracks for the co-linear cracks of pipelines and proposed a strain-based crack tip opening displacement estimation method for evaluating the interactions between co-linear double cracks. From the above review, it is found that although the factors affecting the interaction between pipeline cracks have been analyzed, the vast majority of articles have considered relatively simple models with one

or two parameters. A comprehensive study on the interaction between cracks on pipelines is needed especially about the shielding or enhancing boundary and extent.

As mentioned above, cracks in pipelines tend to appear in the form of surface multi-cracks or crack clusters. It is important to study the interaction between cracks if the pipeline crack cluster is to be evaluated from a safety point of view. In this paper, two surface cracks inside a pipe were taken into consideration, and the interaction between the cracks in terms of the shielding or enhancing effect on the stress intensity factor of the cracks was studied. The boundary of crack shielding or enhancing interactions was drawn, and the formulas for calculating the stress intensity factor of the double cracks were fitted, which provides important references for the evaluation of double cracks in engineering.

2. Finite Element Modeling and Crack Analysis Software

2.1. Finite Element Model

In this paper, a pipe containing two circumferential parallel internal surface cracks is studied, as shown in Figure 1, and the pipe dimensions as well as the materials are given in Table 1. The pipe is subjected to a uniform distal stress σ = 22.7 MPa at one end, completely fixed at one end, and an internal pressure of p = 10 MPa inside the pipe.

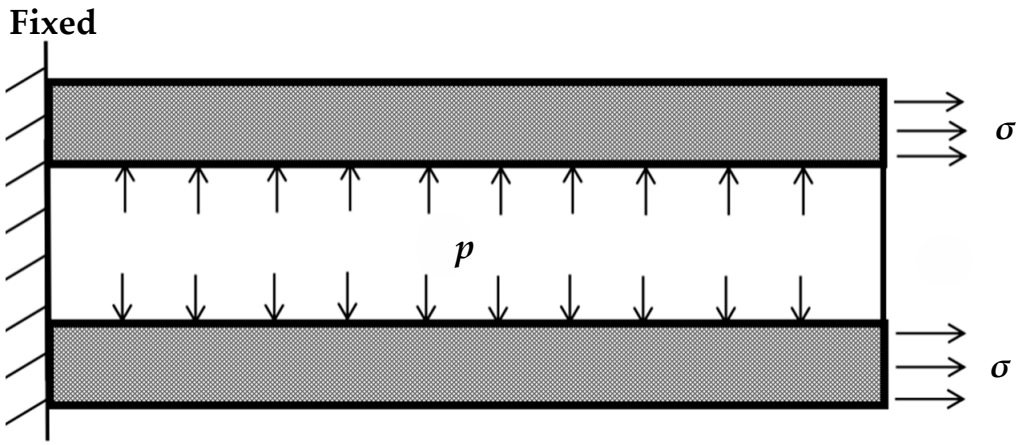

Figure 1. Schematic of pipe loads and constraints.

Table 1. Pipe sizes and materials.

Materials	Young's Modulus	Poisson's Ratio	Inside Diameter	Wall Thickness	Length
S30408	195 GPa	0.3	D (mm)	t (mm)	5(D + 2t) (mm)

Figure 2 shows the schematic diagrams of ring-oriented inner double surface cracks. In Figure 2a, a (mm) is the crack depth; 2l (mm) is the arc length of the crack on the inner surface, which is referred to as the span in this paper. In Figure 2b, two cracks are depicted. The relative long crack with points A, B, and E is called the primary crack, and the other one is called the secondary crack. h (mm) is the spacing, and s (mm) is the offset arc length between cracks. Points A and B are the two endpoints of the primary crack on the inner wall surface; E is the maximum depth point. Clearly, point A is the far point and point B the near point from the secondary crack.

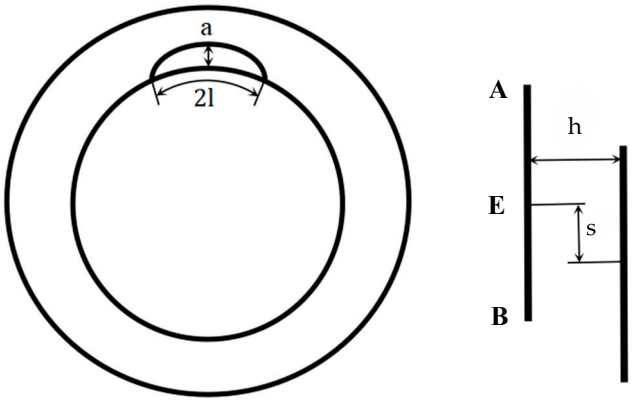

(**a**) (**b**)

Figure 2. Schematic diagrams of cracks: (**a**) crack on the annular inner surface of the pipe; (**b**) double cracks.

2.2. Principles for Evaluating SIF in FRANC3D Crack Analysis Software

FRANC3D—V8.4 crack analysis software calculates the stress intensity factor of a crack based on the M-integral, which has a similar mathematical expression to the J-integral and can realize the superposition of the stress intensity factor for multiple conditions. FRANC3D performs the conservation integral calculation for two unit rings around the crack tip, and the integration domain includes an inner ring of 15-node singular-wedge units and an outer ring of 20-node hexahedral units. The stress intensity factors for the three fracture modes can be calculated identically. The steps and principles of M-integral calculation are as follows.

Calculate the energy release rate G by two ways; on the basis of the Irwin crack closure integral and Williams Extension [37], solve G_1 by material properties and the stress intensity factor, as shown in Equation (1); on the basis of the J-integral [38,39], calculate G_2 by stress, strain, and displacement, as shown in Equation (2), and the calculated area is shown in Figure 3.

$$G_1 = \frac{1-v^2}{E}K_I^2 + \frac{1-v^2}{E}K_{II}^2 + \frac{1+v}{E}K_{III}^2 \tag{1}$$

$$G_2 = \frac{\int_V^0 \left(\sigma_{ij}\frac{\partial u_i}{\partial x_1} - \frac{1}{2}\sigma_{ij}\varepsilon_{ij}\delta_{1j}\right)\frac{\partial q}{\partial x_j}dV}{\int q(s)ds} \tag{2}$$

$$\delta_{1j} = \begin{cases} 1 & (j=1) \\ 0 & (j\neq 1) \end{cases} \tag{3}$$

where E and v are material properties; K is the stress intensity factor; $\sigma_{ij}, \varepsilon_{ij}, u_{ij}$ are stress, strain, and displacement; q is the virtual expansion; and V is the region of the J-integral calculation.

The principle of elastic superposition is that if there is a solution that satisfies the elastic governing equations and it is added to a second solution that satisfies the governing equations, then the result will also satisfy the governing equations. Using the elastic superposition principle, the finite element solution and the analytical solution are superimposed, and the results are as follows:

$$K_I = K_I^{(1)} + K_I^{(2)}, K_{II} = K_{II}^{(1)} + K_{II}^{(2)}, K_{III} = K_{III}^{(1)} + K_{III}^{(2)} \tag{4}$$

$$\sigma_{ij} = \sigma_{ij}^{(1)} + \sigma_{ij}^{(2)}, \varepsilon_{ij} = \varepsilon_{ij}^{(1)} + \varepsilon_{ij}^{(2)}, u_{ij} = u_{ij}^{(1)} + u_{ij}^{(2)} \tag{5}$$

where (1) is the result of the finite element analysis; (2) is the analytic solution. Substituting Equation (4) into Equation (1), Equation (6) is obtained.

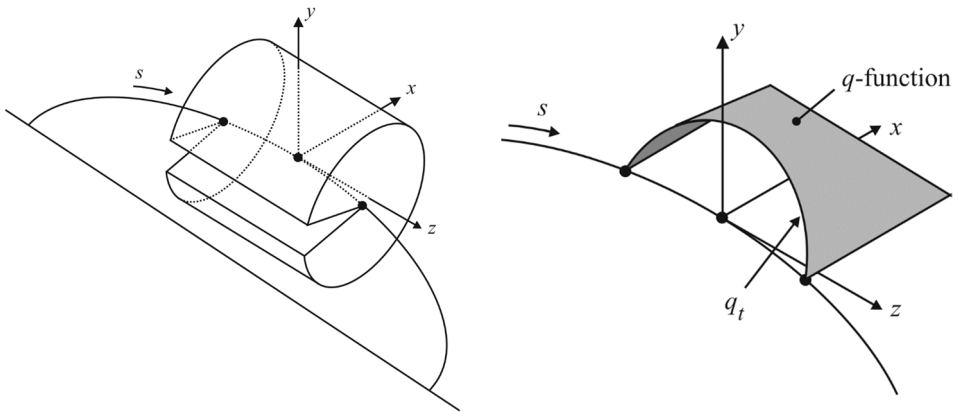

Figure 3. Schematic diagrams of the leading edge of the crack.

$$G = G^{(1)} + G^{(2)} + M^{(1,2)} \tag{6}$$

substituting Equation (4) into Equation (1) yields M equations about the stress intensity factor and material properties, as shown in Equation (7); substituting Equation (5) into Equation (2) yields M equations about stress, strain, and displacement, as shown in Equation (8).

$$M_1^{(1,2)} = \frac{1-v^2}{E} K_I^{(1)} K_I^{(2)} + \frac{1-v^2}{E} K_{II}^{(1)} K_{II}^{(2)} + \frac{1+v}{E} K_{III}^{(1)} K_{III}^{(2)} \tag{7}$$

$$M_2^{(1,2)} = \frac{\int_V^0 \left(\sigma_{ij}^{(1)} \frac{\partial u_i^{(2)}}{\partial x_1} + \sigma_{ij}^{(2)} \frac{\partial u_i^{(1)}}{\partial x_1} - W^{(1,2)} \delta_{1j} \right) \frac{\partial q}{\partial x_j} dV}{\int q(s) ds} \tag{8}$$

setting up $K_I^{(2)} = 1, K_{II} = K_{III} = 0$ yields the formula for K_I, and solving K_{II} and K_{III} follows the same principle.

$$K_I^{(1)} = \frac{E}{1-v^2} \frac{\int_V^0 \left(\sigma_{ij}^{(1)} \frac{\partial u_i^{(2)}}{\partial x_1} + \sigma_{ij}^{(2)} \frac{\partial u_i^{(1)}}{\partial x_1} - W^{(1,2)} \delta_{1j} \right) \frac{\partial q}{\partial x_j} dV}{\int q(s) ds} \tag{9}$$

2.3. FRANC3D Crack Simulation Validation

For pipe circumferential inside surface cracks, API 579-1/ASME FFS-1 2016 Fitness-For-Service [40] gives the empirical formula to evaluate the stress intensity factor:

$$K_I^0 = G_0 \left(\frac{pR_0^2}{R_0^2 - R_i^2} + \frac{F}{\pi \left(R_0^2 - R_i^2 \right)} \right) \sqrt{\pi a / Q} \tag{10}$$

where Q and G_0 are given by API 579-1/ASME FFS-1, F is Net-Section Axial Force. R_i and R_0 are the inner and outer radii of the pipe. In order to verify the accuracy of crack modeling using FRANC3D, the FRANC3D calculation is compared with the empirical calculation of API 579-1/ASME FFS-1, and the results are listed in Table 2.

From Table 2, it is seen that the FRANC3D calculation results agree well with the API 579-1/ASME FFS-1 2016 Fitness-For-Service calculation results with a difference less than 5%, indicating that the stress intensity factor calculation using FRANC3D is reliable and accurate.

Table 2. A comparison of the results by FRANC3D with those of API 579-1/ASME FFS-1.

a/mm	c/mm	D/mm	t/mm	FRANC3D K_1^0 (Point E)	ASME FFS-1 K_1^0 (Point E)	Relative Difference
1	1	50	5	26.78	25.78	3.9%
1	2	50	5	35.93	36.39	1.3%
2	2	50	5	38.46	39.53	2.7%
2	4	50	5	53.09	53.50	0.8%
3	3	50	5	47.28	49.28	4.1%
3	6	50	5	68.54	69.11	0.8%

3. The Simulation of the Interaction between Two Parallel Cracks

In this section, the variation in the stress intensity factors of two parallel cracks with different sizes and different relative positions on the pipe under internal pressure is investigated. The variables include the distance and offset between the double cracks and the depth and span of the sub-cracks. Specifically, the SIFs at three points, A, B, and C, at the leading edge of the crack is used to study the interaction between the cracks. In this paper K_I/K_I^0 are used to express the magnitude of inter-crack interactions, where K_I is the finite element calculation value of the stress intensity factor at the point of the leading edge of the primary crack under the influence of the secondary crack, and K_I^0 is the stress intensity factor at the point of the leading edge of the primary crack in the absence of the secondary crack. If K_I/K_I^0 is greater than 1, the crack interaction is reinforcing and vice versa for shielding. In the following Sections 3.1 and 3.2, the pipe size is kept constant as $D = 50$ mm, $t = 5$ mm; the primary crack is used as the reference crack with the size kept constant as $2l_1 = 8$ mm, $a = 2$ mm, while the location and size of the secondary crack are changed for analysis.

3.1. The Effects of the Spacing and Offset between Cracks

In this subsection, the primary and secondary cracks are of the same size, and the position of the primary crack is fixed, while the location of the secondary crack is changing. The numerical simulation results are shown in Figure 4, where the red rectangular areas are the crack leading edge point corresponding to the figure.

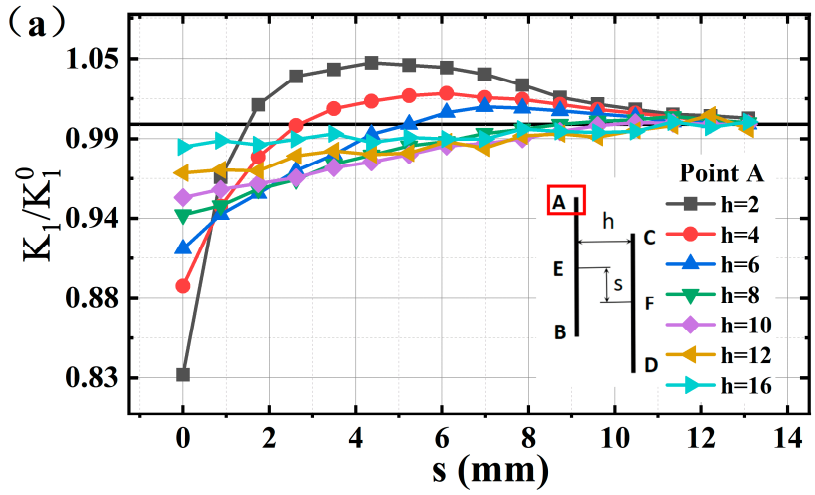

Figure 4. *Cont.*

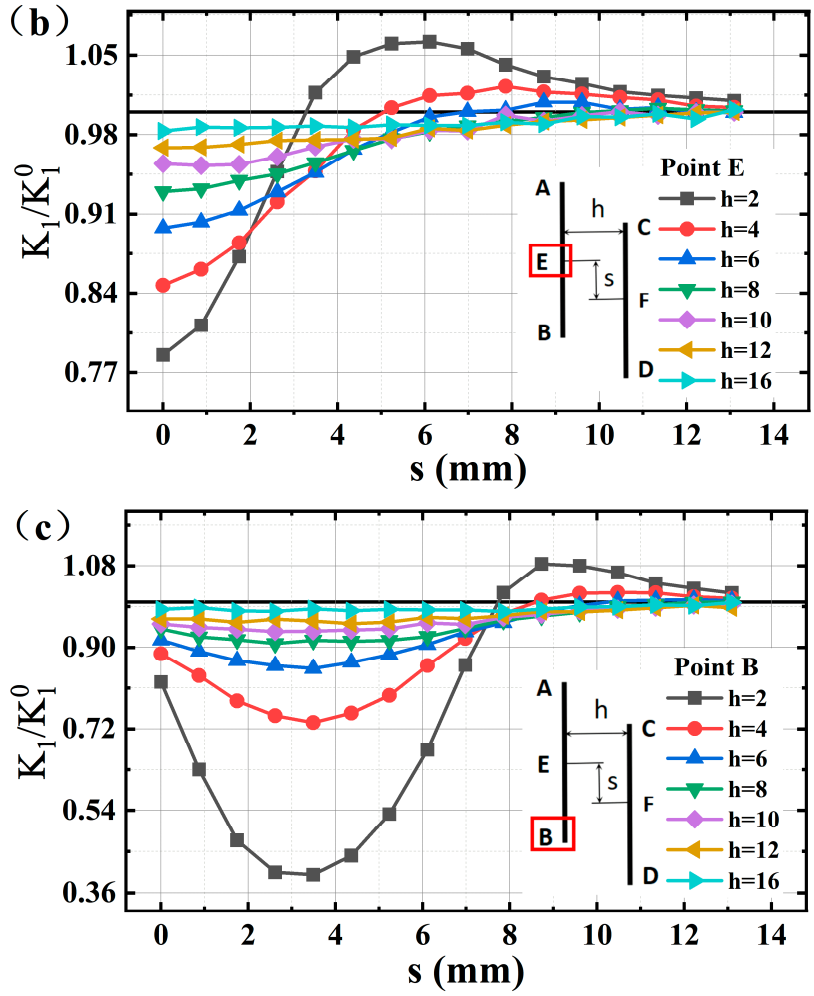

Figure 4. Variation in K_I/K_I^0 with s for different h(mm): (**a**) point A; (**b**) point E; and (**c**) point B.

Figure 4 gives the K_I/K_I^0 variation with s at points A, B, and E of the crack leading edge at different intervals. It is seen that when the spacing h increases, the shielding effect gradually decreases, and the interaction finally disappears if spacing h is large enough. The change in K_I/K_I^0 with the offset s is relatively complex. When the main crack overlaps the secondary crack in axial projection, the interaction is shielding on the point of the leading edge and vice versa. On the contrary, if the two cracks are not overlapped, or in other words, the two cracks are offset, their interactions tend to be enhancement. Of course, if the offset s is large compared to crack size, their interactions will also disappear. Taking the proximal point B at h = 2 mm as an example, when the offset s changes from 0 to 8 mm, the proximal point B is under the shielding effect, and the magnitude of the shielding effect is closely related to the depth of the secondary cracks at the axial overlapping on the proximal point B. The proximal point B is subjected to the enhancement effect when the offset exceeds 8 mm where the secondary crack does not overlap with the axial projection of the proximal point B. When offset s exceeds 12, the enhancement effect almost disappears, meaning the two cracks do not interact with each other.

3.2. The Effects of the Secondary Crack Size

In this subsection, the locations for the two cracks and the primary crack size are fixed, but the size of the secondary crack varies to see its influence on the primary crack. Two dimensionless numbers R_a and R_l are defined to indicate the relative dimensions of the cracks, $R_a = a_2/a_1$, $R_l = l_2/l_1$, where a_2 is the secondary crack depth, a_1 is the primary

crack depth, l_2 is the secondary crack span, and l_1 is the primary crack span. The numerical simulation results are shown in Figure 5.

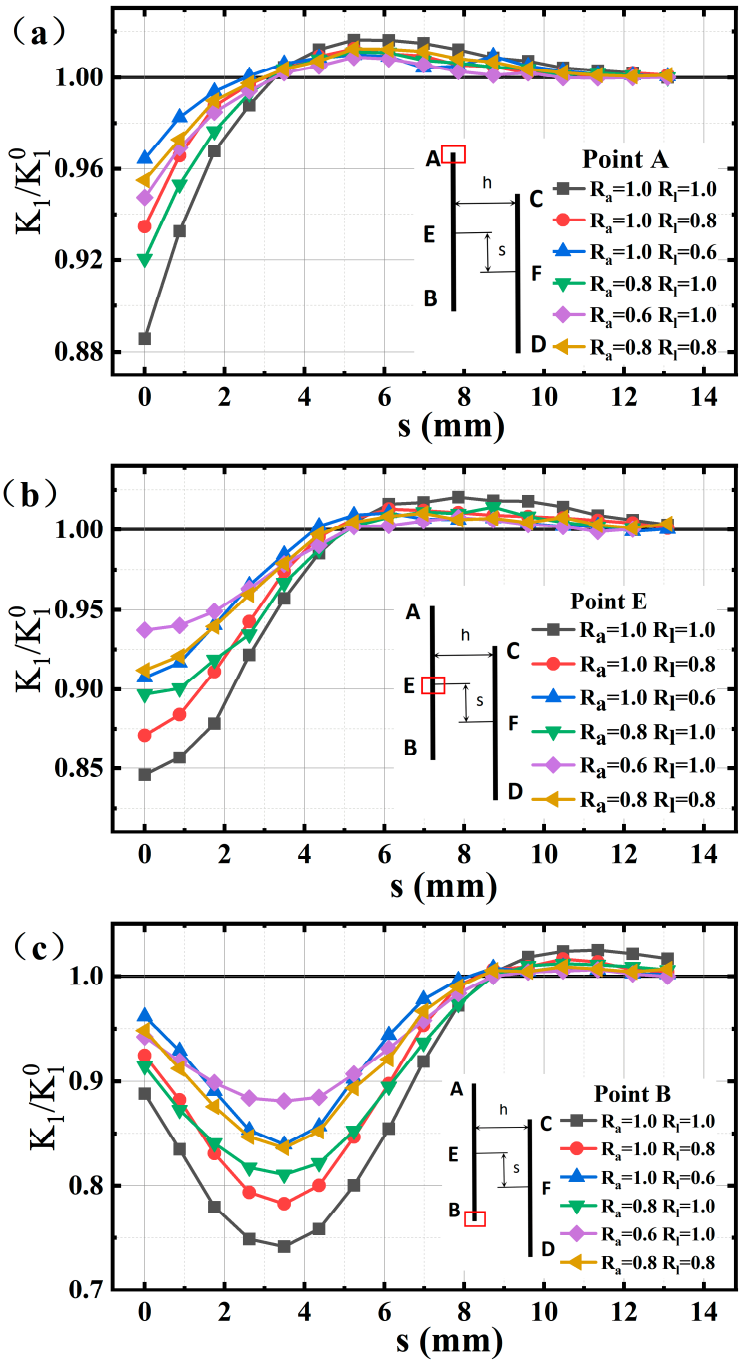

Figure 5. Variation in K_I/K_I^0 with s for different R_a and R_l: (**a**) point A; (**b**) point E; and (**c**) point B.

It is seen that the changing of the secondary crack size does not change the variation trend of K_I/K_I^0 with s. The enhancement or shielding behaviors on the primary crack stay the same, but the magnitude of the enhancement or shielding effect varies with the crack size.

3.3. Effect of Pipe and Primary Crack Size

In the above analysis, the pipe size is fixed as D = 50 mm and t = 5 mm, the pipe load is fixed as σ = 22.7 MPa and p = 10 MPa, and the primary crack size is fixed as $2l_1$ = 8 mm

and a = 2 mm. In this subsection, the effects of the pipe size, the pipe load, and the primary crack size on K_I/K_I^0 are studied.

Figure 6 shows the variation in K_I/K_I^0 at point A with offset s for different D and t. It is seen that the effect of changing D and t on K_I/K_I^0 is neglectable. In fact, the pipe size may affect K_I and K_I^0 but has less effect on the interaction between cracks, so the effect caused by the pipe size will not be considered in the following study of this paper.

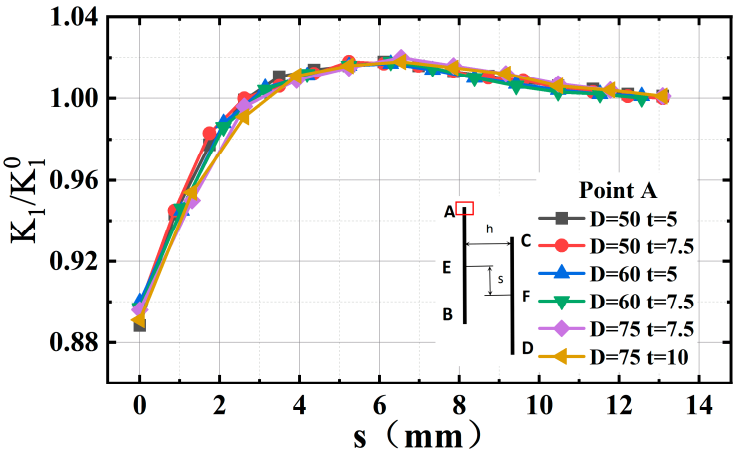

Figure 6. Variation in K_1/K_1^0 at point A with s for different D and t.

Figure 7 shows the variation in K_I with offset s at point A for different internal pressure p and corresponding distal stress σ. It is seen that as expected, the pipe load determines K_I, but for K_I/K_I^0, which reflects the crack interactions, the pipe load has no effects, as shown in Figure 8.

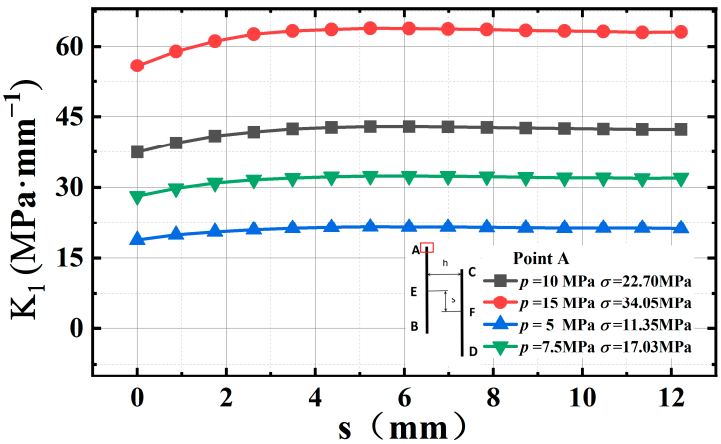

Figure 7. Variation in K_1 at point A with s for different p and σ.

Figure 9 shows the effect of the primary crack size on the interaction between cracks where a_1 and $2l_1$ of the primary crack are changed, while R_a, R_l, and the pipe size are kept constant. Two dimensionless numbers $H_l = h/2l_1$, $S_l = s/2l_1$ are defined in order to keep the spacing h and offset s varying with the crack size, H_l is the relative spacing between cracks, and S_l is the relative bias between cracks. It is seen from Figure 6 that when $a \leq 0.5t$, the change in the primary crack size has little effect on the crack interactions if the position between the two cracks is proportionally changed.

In summary, the finite element simulation results based on a specific pipe and primary crack size can be applied to other pipe and primary crack sizes if the relative spacing and offset are kept the same.

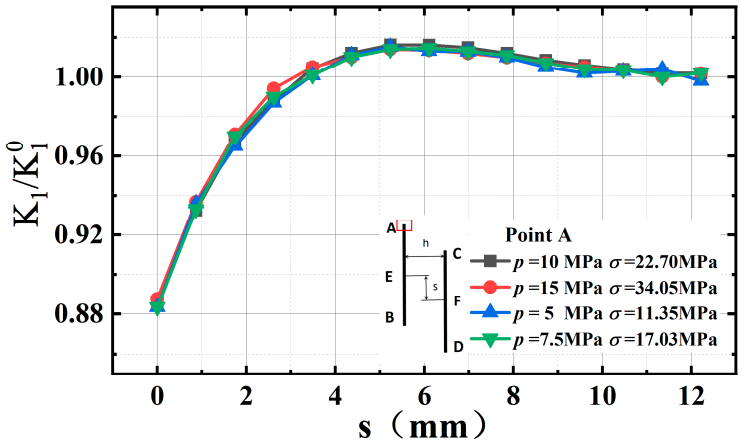

Figure 8. Variation in K_1/K_1^0 at point A with s for different p and σ.

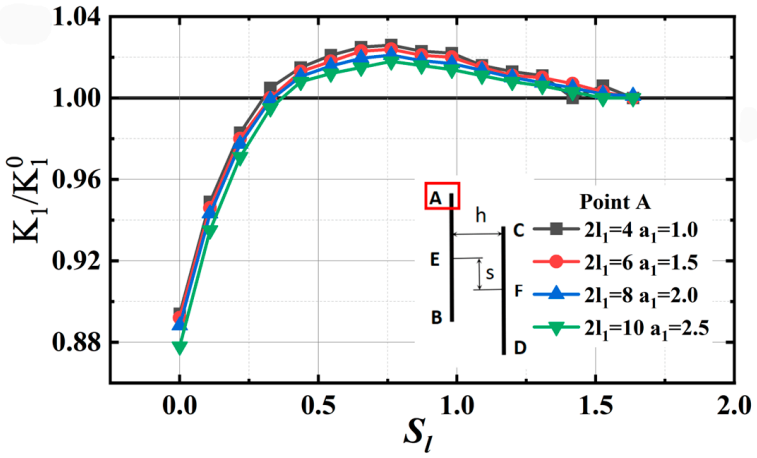

Figure 9. Variation in K_1/K_1^0 with S_l for different a_1 and $2l_1$ at point A.

3.4. Boundaries for Shielding or Enhancing Interaction

Based on the numerical simulation results, boundaries for shielding or enhancing interaction between the two parallel cracks can be drawn, as shown in Figure 10. It is seen that when H_l or S_l is large enough, i.e., the two cracks are far from each other, no interactions occur. If H_l is relatively small and S_l is relatively large, i.e., the two cracks are closely offset, the interactions between them are more likely enhancement, especially for endpoint A.

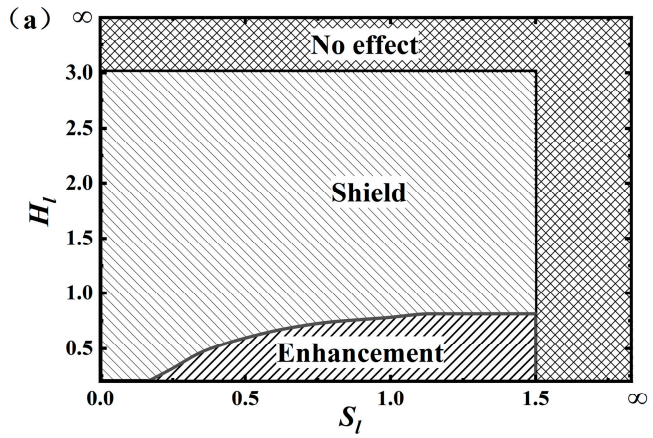

Figure 10. *Cont.*

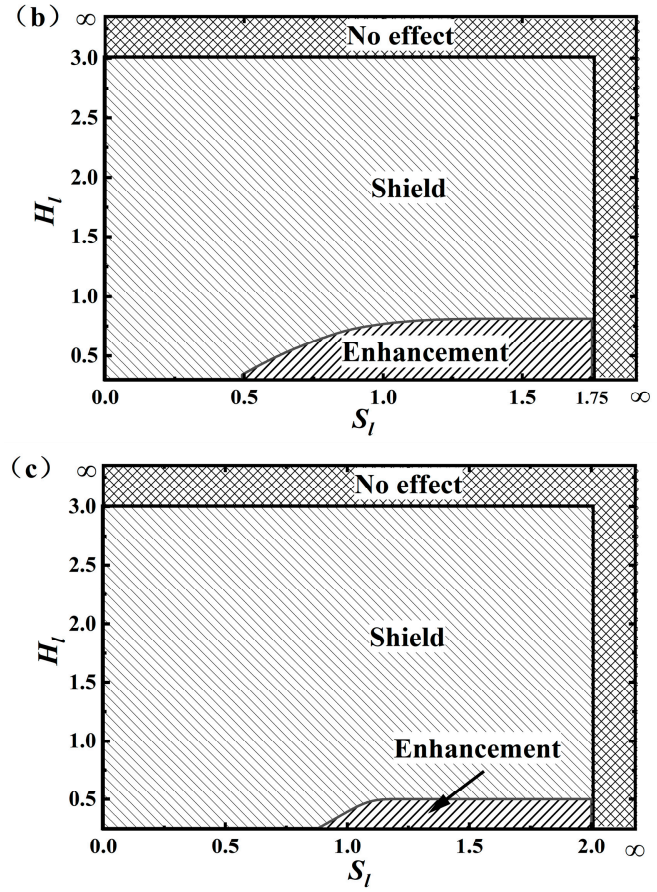

Figure 10. Boundaries for shielding or enhancing interaction between the two cracks: (**a**) point A; (**b**) point E; and (**c**) point B.

4. Empirical Equations for Calculating Stress Intensity Factors of Crack

The above analysis reveals that the interaction between the two cracks is controlled by their relative locations and crack size. In this section, based on enough numerical simulation results, the equations for calculating the stress intensity factor of the primary crack were fitted as a function of relative spacing $H_l = h/2l_1$, offset $S_l = s/2l_{1.}$, and relative crack size $R_a = a_2/a_1$, $R_l = l_2/l_1$, and the results are listed in Tables 3–5.

The above equations are applicable to any length and diameter pipeline, but the crack depth should not exceed fifty percent of the wall thickness with the ratio of the crack depth to the span being 1:4. It turns out that when S_l is greater than 2 or H_l is greater than 3, there is little relative interaction between the double cracks, so K_I/K_I^0 is approximately equal to 1.

The above formulas quantitatively characterize the interaction between cracks. They are useful in engineering when equalizing the multi-cracks into a single crack or performing crack fatigue propagation calculation for the safety assessment of the pipelines containing cracks.

In order to validate the accuracy and applicability of the empirical equations obtained above for calculating K_I/K_I^0, both equation calculation and the finite element simulation for some other double cracks within the range corresponding to the equation are performed and compared. The results are listed in Table 6. It is seen that the results of the empirical equation calculation and the finite element simulation agree well with each other with a maximum relative difference less than 4%, meaning that the equations are accurate enough in engineering application.

Table 3. Empirical equations for calculating SIFs at point A.

Steps		Formulas
δ_1	$0.25 < H_l \leq 1$	$S_l \leq 0.87H_l + 0.33$, $\delta_1 = A_1 - B_1 * {C_1}^{18.35S_l}$ $A_1 = 1.05 - 0.032H_l + 0.018{H_l}^2$ $B_1 = 0.31 - 0.43H_l + 0.23{H_l}^2$ $C_1 = 0.37 + 1.03H_l - 0.46{H_l}^2$
		$S_l > 0.87H_l + 0.33$, $\delta_1 = 1 + \frac{A_1 - 1}{1 + 10^{C_1(B_1 - 18.35S_l)}}$ $A_1 = 1.07 - 0.13H_l - 0.062{H_l}^2$ $B_1 = 18.61 + 2.17H_l + 4.35{H_l}^2$ $C_1 = -0.1 - 0.02H_l - 0.21{H_l}^2$
	$1 < H_l \leq 3$	$\delta_1 = \frac{18.35(1 - A_1)S_l}{30} + A_1 A_1 = 0.85 + 0.1H_l - 0.018{H_l}^2$
δ_2		$\delta_2 = A_2 + B_2 R_l + C_2 {R_l}^2$ $A_2 = 0.99 - 0.011R_a$ $B_2 = -0.037 + 0.1R_a$ $C_2 = 0.073 - 0.23R_a$
$\frac{K_I}{K_I^0}$		$\frac{K_I}{K_I^0} = 1 - (1 - \delta_2)(1 - \delta_1)/0.1117$

Table 4. Empirical equations for calculating SIFs at point E.

Steps		Formulas
δ_1	$0.25 < H_l \leq 1$	$S_l \leq 0.87H_l + 0.545$, $\delta_1 = A_0 + \frac{A_1 - A_0}{1 + 10^{C_1(B_1 - 18.35S_l)}}$ $A_0 = 0.69 + 0.36H_l - 0.13{H_l}^2$ $A_1 = 1.12 - 0.262H_l + 0.14{H_l}^2$ $B_1 = 3.37 + 7.66H_l - 1.82{H_l}^2$ $C_1 = 0.33 - 0.37H_l + 0.148{H_l}^2$
		$S_l > 0.87H_l + 0.545$, $\delta_1 = 1 + \frac{A_1 - 1}{1 + 10^{C_1(B_1 - 18.35S_l)}}$ $A_1 = 1.18 - 0.39H_l + 0.218{H_l}^2$ $B_1 = 14.49 + 9.61H_l + 2.718{H_l}^2$ $C_1 = -0.15 + 0.36H_l - 0.522{H_l}^2$
	$1 < H_l \leq 3$	$\delta_1 = \frac{18.35(1 - A_1)S_l}{30} + A_1$, $A_1 = 1 - 0.32 * 0.83^{8H_l}$
δ_2		$\delta_2 = A_2 + B_2 R_l$ $A_2 = 0.98 - 0.015R_a + 0.048{R_a}^2$ $B_2 = 0.038 - 0.066R_a - 0.14{R_a}^2$
$\frac{K_I}{K_I^0}$		$\frac{K_I}{K_I^0} = 1 - (1 - \delta_2)(1 - \delta_1)/0.1530$

Table 5. Empirical equations for calculating SIFs at point B.

Scheme		Formulas
δ_1	$0.25 < H_l \leq 1.25$	$0 \leq S_l \leq 0.81$, $\delta_1 = A_1 + 4.59(B_1 - A_1)S_l + 5.26(A_1 - B_1){S_l}^2$ $A_1 = 0.756 + 0.31H_l - 0.125{H_l}^2$ $B_1 = 0.95 - 1.37 * 0.632^{8H_l}$
		$0.81 < S_l \leq 0.87H_l + 0.87$, $\delta_1 = A_1 + B_1 S_l + C_1 {S_l}^2$ $A_1 = 0.78 - 24.01 * 0.44^{8H_l}$ $B_1 = 0.255 - 48.21 * 0.425^{8H_l}$ $C_1 = -0.077 + 24.14 * 0.41^{8H_l}$
		$S_l > 0.87H_l + 0.87$,$\delta_1 = A_1 + \frac{A_0 - A_1}{1 + e^{(18.35S_l - B_1)/C_1}}$ $A_0 = 1.20 - 0.55H_l + 0.383{H_l}^2$ $A_1 = 1.01 - 0.023H_l + 0.0134{H_l}^2$ $B_1 = 25.65 - 3.03H_l + 12.57{H_l}^2$ $C_1 = 1.34 + 3.6H_l - 5.894{H_l}^2$
	$1.25 < H_l \leq 3$	$\delta_1 = \frac{18.35(1 - A_1)S_l}{34} + A_1$, $A_1 = 1.005 - 0.213 * 0.868^{8H_l}$

Table 5. *Cont.*

Scheme	Formulas
δ_2	$\delta_2 = A_2 + B_2 R_a + C_2 {R_a}^2$ $A_2 = 0.85 + 0.31R_l - 0.31R_l^2$ $B_2 = 0.2 - 0.37R_l + 0.19R_l^2$ $C_2 = -0.11 + 0.2R_l - 0.23R_l^2$
$\frac{K_I}{K_I^0}$	$\frac{K_I}{K_I^0} = 1 - (1 - \delta_2)(1 - \delta_1)/0.1139$

Table 6. Accuracy validation for the empirical equations.

D	t	$2l_1$	a	R_l	R_a	H_l	Average Difference	Maximum Difference
50	5	8	2	1	1	5.5	1.01%	2.22%
50	5	8	2	1	1	9	0.85%	1.48%
50	5	8	2	0.85	0.95	3	1.13%	1.51%
50	5	8	2	0.5	0.7	6	0.92%	1.82%
70	15	8	2	1	1	4	1.83%	3.32%
80	20	12	3	0.8	0.8	2	1.85%	3.62%
50	5	4	1	0.75	0.75	3	1.94%	2.74%
500	50	80	20	1	1	4	1.41%	2.27%

5. Conclusions

In this paper, the interaction between annular parallel double cracks on the inner surface of a pressure pipeline was investigated based on the FRANC3D crack simulation. Conclusions are drawn as follows.

(1) The interaction between the two cracks is mainly controlled by the locations between them. The interaction could be shielding or reinforcing.

(2) If there is no offset between the double cracks, the crack leading edge is shielded, and the smaller the spacing is, the stronger the shielding effect is. If offset occurs and the spacing is not so large between the double cracks, the distal end of the cracks is generally subjected to the reinforcing interaction, while the proximal end of the cracks is generally subjected to the shielding effect.

(3) The relative sizes of the cracks do not change the boundaries of enhancement or shielding but affect the magnitude of the enhancement or shielding. The effect of pipe size and load on crack interaction can be neglected. When $a \leq 0.5t$, the change in the primary crack size has little effect on the crack interactions if the position between the two cracks is proportionally changed.

(4) For the circumferential parallel double cracks on the inner surface of a pipeline under internal pressure, boundaries for shielding or enhancing interactions and empirical equations for calculating the stress intensity factor of the primary crack were obtained based on sufficient numerical simulation results.

Author Contributions: Conceptualization, C.Q. and H.L.; Data curation, J.C.; Formal analysis, J.C. and C.Q.; Investigation, J.C.; Methodology, Z.W. and H.L.; Project administration, C.Q. and H.L.; Software, J.C.; Supervision, C.Q., H.L. and Z.W.; Validation, J.C. and C.Q.; Writing—original draft, J.C.; Writing—review and editing, C.Q. and H.L. All authors have read and agreed to the published version of the manuscript.

Funding: National Key Research and Development Program of China (Grant No. 2023YFC3010500) and the Fundamental Research Funds for the Central Universities (ZY2409).

Institutional Review Board Statement: Not applicable.

Informed Consent Statement: Not applicable.

Data Availability Statement: Data are contained within the article.

Conflicts of Interest: The authors declare no conflicts of interest.

References

1. Shao, J.; Zhang, Q. Analysis of the causes of cracks in pressure pipelines and preventive measures. *Pet. Chem. Equip.* **2011**, *14*, 10–12.
2. Irwin, G.R. Analysis of stresses and strains near end of a crack traversing a plate. *J. Appl. Mech.* **1957**, *24*, 361–364. [CrossRef]
3. Mechab, B.; Malika, M.; Mokadem, S.; Boualem, S. Probabilistic elastic-plastic fracture mechanics analysis of propagation of cracks in pipes under internal pressure. *Fract. Struct. Integr.* **2020**, *14*, 202–210. [CrossRef]
4. Tan, X.; Wang, G.; Tu, S.; Xuan, F. Comparisons of creep constraint and fracture parameter C* of different types of surface cracks in pressurized pipes. *Int. J. Press. Vessel. Pip.* **2019**, *172*, 360–372. [CrossRef]
5. Salem, M.; Mechab, B.; Berrahou, M.; Bouiadjra, B.B.; Serier, B. Failure Analyses of Propagation of Cracks in Repaired Pipe under Internal Pressure. *J. Fail. Anal. Prev.* **2019**, *19*, 212–218. [CrossRef]
6. Luis, E.; Antonio, J.B.; Sourojeet, C.; Daniela, G. Comparison of the Stress Intensity Factor for a Longest Crack in an elliptical Base Gas Pipe, using FEM vs. DCT method. *Forces Mech.* **2023**, *13*, 100233.
7. Seenuan, P.; Noraphaiphipaksa, N.; Kanchanomai, C. Stress Intensity Factors for Pressurized Pipes with an Internal Crack: The Prediction Model Based on an Artificial Neural Network. *Appl. Sci.* **2023**, *13*, 11446. [CrossRef]
8. Yao, X.M.; Zhang, Y.C.; Pei, Q.; Jin, L.Z.; Ma, T.H.; He, X.H.; Zhou, C.Y. Empirical Solution of Stress Intensity Factors for the Inclined Inner Surface Crack of Pipe under External Pressure and Axial Compression. *Materials* **2022**, *16*, 364. [CrossRef] [PubMed]
9. Kumar, S.S.; Balaji, N.V. Mode-I, Mode-II, and Mode-III Stress Intensity Factor Estimation of Regular- and Irregular-Shaped Surface Cracks in Circular Pipes. *J. Fail. Anal. Prev.* **2020**, *20*, 1–15.
10. Fu, G.; Yang, W.; Li, C. Stress intensity factors for mixed mode fracture induced by inclined cracks in pipes under axial tension and bending. *Theor. Appl. Fract. Mech.* **2017**, *89*, 100–109. [CrossRef]
11. Qiu, K.; Du, P.; Wei, X.; Qu, Y.; Chen, N. Fracture phase-field method-based circumferential surface crack propagationinvestigation of pipeline. *Chin. J. Ship Res.* **2024**, *19*, 1–8. (In Chinese) [CrossRef]
12. Zhou, Z.J.; Wen, D.; Len, X.F. Study on the stress intensity factor of pipeline outer surface cracks. *Mod. Mach.* **2024**, 36–41. [CrossRef]
13. Cui, Y.Y.; Li, H.F.; Qian, C.F.; Wu, Z. Calculation of stress intensity factor for pipe penetration diagonal cracks. *Press. Vessel* **2023**, *40*, 30–36+66.
14. Chen, F.; Ding, N.; Wang, X.Y.; Zhang, F.; Liu, G. Numerical simulation of pipeline surface crack circumferential extension based on XFEM. *Mater. Prot.* **2022**, *55*, 47–54+78.
15. Li, Z.; Jiang, X.; Hopman, H. Surface Crack Growth in Offshore Metallic Pipes under Cyclic Loads: A Literature Review. *J. Mar. Sci. Eng.* **2020**, *8*, 339. [CrossRef]
16. Tanwar, A.; Das, S.; Craciun, E. Interaction among interfacial offset cracks in composite materials under the anti-plane shear loading. *ZAMM-J. Appl. Math. Mech.* **2023**, *103*, 202300081. [CrossRef]
17. Anis, F.S.; Koyama, M.; Hamada, S.; Noguchi, H. Simplified stress field determination for an inclined crack and interaction between two cracks under tension. *Theor. Appl. Fract. Mech.* **2020**, *107*, 102561. [CrossRef]
18. Shen, Q.Q.; Rao, Q.H.; Li, Z.; Yi, W.; Sun, D.L. Interacting mechanism and initiation prediction of multiple cracks. *Trans. Nonferrous Met. Soc. China* **2021**, *31*, 779–791. [CrossRef]
19. Wang, Y.X.; Javadi, A.; Corrado, F. Analysis of Interaction of Multiple Cracks Based on Tip Stress Field Using Extended Finite Element Method. *J. Appl. Math.* **2022**, *2022*, 1010174. [CrossRef]
20. Long, H.; Tuan, T.N. Facilitation effect of multiple crack interaction on fatigue life reduction and a quantitative evaluation of interactions factor of two parallel Non-coplanar cracks. *Theor. Appl. Fract. Mech.* **2023**, *125*, 103941.
21. Parsania, A.; Kakavand, E.; Hosseini, A.S.; Parsania, A. Estimation of multiple cracks interaction and its effect on stress intensity factors under mixed load by artificial neural networks. *Theor. Appl. Fract. Mech.* **2024**, *131*, 104340. [CrossRef]
22. Han, Z.C. Research on Inter-Crack Interactions and Crack Population Equivalence Method. Ph.D. Dissertation, Beijing University of Chemical Technology, Beijing, China, 2021.
23. Zhang, R.; Han, Y. Study on the interference effect of crack strength factor on inner surface of pipeline based on ANSYS Workbench. *Electromech. Eng. Technol.* **2023**, *52*, 177–180+189.
24. Huang, Y.F.; Qiu, J.H.; Guo, Z.Q. Boundary element analysis of fracture behavior under multi-crack interaction. *Sci. Technol. Eng.* **2018**, *18*, 6–12.
25. Cui, W.; Xiao, Z.M.; Zhang, Q.; Yang, J.; Feng, Z.M. Modeling the Crack Interference in X80 Oil and Gas Pipeline Weld. *Materials* **2023**, *16*, 3330. [CrossRef] [PubMed]
26. Yao, A.L.; He, W.; Xu, T. 3D-VCCT based fracture analysis method for gas pipelines with multiple cracks. *Nat. Gas Ind. B* **2019**, *6*, 488–496. [CrossRef]
27. Hamzah, K.; Long, N.N.; Senu, N. Stress intensity factor for multiple cracks in bonded dissimilar materials using hypersingular integral equations. *Appl. Math. Model.* **2019**, *73*, 95–108. [CrossRef]
28. Xie, M.J.; Wang, Y.F.; Xiong, W.N.; Zhao, J.L.; Pei, X.J. A Crack Propagation Method for Pipelines with Interacting Corrosion and Crack Defects. *Sensors* **2022**, *22*, 986. [CrossRef] [PubMed]
29. Sahnoun, M.; Ouinas, D.; Bouiadjra, B.B.; Olay, J.V. Numerical Modelling of the Interaction Macro–Multimicrocracks in a Pipe under Tensile Stress. *Adv. Mater. Res.* **2015**, *1105*, 245–250. [CrossRef]

30. Chong, Z.W.; Ma, T.X.; Yu, D.L.; Wu, D.R.; Tao, J.; Lv, H. Stress Intensity Factor of Double Cracks on Seabed-Spanning Pipeline Surface under the Spring Boundary. *J. Pipeline Syst. Eng. Pract.* **2021**, *12*, 04021052. [CrossRef]
31. He, X.; Qin, X.; Xie, L. Influence of pipe axial double crack angle on tip stress intensity factor. *J. Northeast. Univ. (Nat. Sci. Ed.)* **2011**, *32*, 1623–1626.
32. Yu, J.; Guo, S.; Wu, Z. Analysis of fatigue life of submarine pipelines containing double crack defects. *China Offshore Platf.* **2016**, *31*, 66–72.
33. Li, W.; Tan, Y.; Wu, W. Effect of two-crack interaction on the stress intensity factor of pipelines. *Oil Gas Storage Transp.* **2019**, *38*, 1125–1129.
34. Wei, M. Research on multi-crack interaction and effect on strength of its main steam pipeline. *China Spec. Equip. Saf.* **2019**, *35*, 70–75.
35. Qin, Y.; Qin, X.; Chen, Z. Study on the influence law between parallel biaxial cracks on the inner surface of thick-walled cylinders. *Electromech. Eng.* **2022**, *39*, 276–280.
36. Zhang, Y.; Fan, M.; Xiao, Z. Nonlinear elastic-plastic stress investigations on two interacting 3-D cracks in offshore pipelines subjected to different loadings. *AIMS Mater. Sci.* **2016**, *3*, 1321–1339. [CrossRef]
37. Williams, L.M. On the Stress Distribution at the Base of a Stationary Crack. *J. Appl. Mech.* **1957**, *24*, 109–114. [CrossRef]
38. Rice, J.R. A Path independent integral and the approximate analysis of strain concentrations by notches and cracks. *J. Appl. Mech.* **1968**, *35*, 379–386. [CrossRef]
39. Rice, J.R.; Rosengren, G.F. Plane strain deformation near crack tip in a power-law hardening material. *J. Mech. Phys. Solids* **1968**, *16*, 1–12. [CrossRef]
40. *API 579-1/ASME FFS-1*; Fitness-for-Service. American Petroleum Institute: Houston, TX, USA, 2016.